Simulating quantum interference in spontaneous decay near plasmonic nanostructures: Population dynamics

Sofia Evangelou, Vassilios Yannopapas,* and Emmanuel Paspalakis
Materials Science Department, School of Natural Sciences, University of Patras, GR-265 04 Patras, Greece
(Received 17 December 2010; published 26 May 2011)

It has been recently shown that the placement of a three-level V-type quantum emitter in the proximity of metallic nanostructures can create dynamics similar to that of quantum interference in spontaneous emission. Here we continue this work and present results on the population dynamics of a three-level V-type quantum emitter for various initial conditions in the presence of a two-dimensional array of metal-coated dielectric nanospheres.

DOI: 10.1103/PhysRevA.83.055805 PACS number(s): 42.50.Nn, 42.50.Ct, 73.20.Mf, 78.67.Bf

For several years it has been realized that the spontaneous emission of quantum emitters, such as atoms, molecules and quantum dots, can be strongly influenced by the presence of nanostructures (for reviews see, e.g., [1,2]). An important effect in such systems is the significantly modified spontaneous decay rate in different emitter dipole moment directions, for example, for orthogonal dipole directions. Agarwal [3] showed that this effect can be used for simulating quantum interference effects in spontaneous emission [4–15]. He proposed to place a three-level quantum emitter with orthogonal dipole moments within or near a structure which suppresses spontaneous emission for a specific dipole orientation. Applying this idea, it has been recently shown [16], by using a rigorous electromagnetic (EM) Green's tensor technique [17–19], that the placement of a three-level V-type quantum emitter in the proximity of simple, or complex, metallic nanostructures can boost the degree of quantum interference in spontaneous emission.

Here we continue this work and present results on the population dynamics of a three-level V-type quantum emitter for different initial conditions in the presence of a two-dimensional array of metal-coated dielectric nanospheres. We also note that quite recently, Hatef and Singh have studied the effects of spontaneous emission interference in absorption and dispersion in metallic photonic crystals doped with quantum dots in the V-type configuration [20]. In addition, the study of spontaneous emission and resonance fluorescence of quantum emitters near various plasmonic structures has attracted significant attention recently [21–28].

The quantum system of interest is shown in Fig. 1(a). We consider a V-type system with two degenerate Zeeman sublevels for the upper states $|2\rangle$ and $|3\rangle$, and one lower state $|1\rangle$. The quantum system is located in vacuum at distance d from the surface of the plasmonic nanostructure. The dipole moment operator is taken as $\vec{\mu} = \mu(|2\rangle\langle 1|\hat{\varepsilon}_- + |3\rangle\langle 1|\hat{\varepsilon}_+) +$ H.c., where $\hat{\varepsilon}_\pm = (\mathbf{e}_z \pm i\mathbf{e}_x)/\sqrt{2}$ describes the right-rotating ($\hat{\varepsilon}_+$) and left-rotating ($\hat{\varepsilon}_-$) unit vectors and μ is taken to be real. Both excited levels $|2\rangle$ and $|3\rangle$ decay spontaneously to the lower level with decay rate 2γ.

The spontaneous decay dynamics in the above system is studied by a density-matrix approach. By considering solely spontaneous emission effects, the time-dependent density matrix equations describing the interaction of the atom with its environment, in the rotating-wave and Weisskopf-Wigner approximations, are given by [16,29–32] (we take $\hbar = 1$)

$$\dot{\rho}_{22} = -2\gamma\rho_{22} - \kappa(\rho_{23} + \rho_{32}), \tag{1}$$

$$\dot{\rho}_{33} = -2\gamma\rho_{33} - \kappa(\rho_{32} + \rho_{23}), \tag{2}$$

$$\dot{\rho}_{23} = -2\gamma\rho_{23} - \kappa(\rho_{22} + \rho_{33}), \tag{3}$$

with $\rho_{11} + \rho_{22} + \rho_{33} = 1$ and $\rho_{nm} = \rho^*_{mn}$. Here κ describes the coupling coefficients between states $|2\rangle$ and $|3\rangle$ due to spontaneous emission in a modified anisotropic vacuum [3], and it is responsible for the effects of quantum interference.

The values of γ and κ are obtained by [29]

$$\gamma = \mu^2\omega_0^2\hat{\varepsilon}_- \cdot \mathrm{Im}\mathbf{G}(\mathbf{r},\mathbf{r};\omega_0)\cdot\hat{\varepsilon}_+ \tag{4}$$

$$\kappa = \mu^2\omega_0^2\hat{\varepsilon}_+ \cdot \mathrm{Im}\mathbf{G}(\mathbf{r},\mathbf{r};\omega_0)\cdot\hat{\varepsilon}_+ . \tag{5}$$

Here, $\mathbf{G}(\mathbf{r},\mathbf{r}';\omega)$ is the dyadic EM Green's tensor that obeys the equation

$$\nabla\times\nabla\times\mathbf{G}(\mathbf{r},\mathbf{r}';\omega) - \frac{\epsilon(\mathbf{r},\omega)\omega^2}{c^2}\mathbf{G}(\mathbf{r},\mathbf{r}';\omega) = \mathbf{I}\delta(\mathbf{r}-\mathbf{r}') . \tag{6}$$

Also, $G_{ij}(\mathbf{r},\mathbf{r}';\omega)$, with $i,j = x,y,z$, are the components of the Green's tensor and $\mathbf{I} = \mathbf{e}_x\mathbf{e}_x + \mathbf{e}_y\mathbf{e}_y + \mathbf{e}_z\mathbf{e}_z$ is the unit dyad (unit tensor). In addition, $\epsilon(\mathbf{r},\omega)$ is the spatially and frequency-dependent dielectric function of the system, $\mathbf{r}$ refers to the position of the quantum emitter, ω_0 is the resonance frequency between states $|1\rangle$ and $|2\rangle$ (or $|3\rangle$), and c is the speed of light in the vacuum.

From Eqs. (4) and (5) we finally obtain the values of γ and κ as [29–33]

$$\gamma = \tfrac{1}{2}\mu^2\omega_0^2\mathrm{Im}[G_\perp(\mathbf{r},\mathbf{r};\omega_0) + G_\parallel(\mathbf{r},\mathbf{r};\omega_0)] = \tfrac{1}{2}(\Gamma_\perp + \Gamma_\parallel), \tag{7}$$

$$\kappa = \tfrac{1}{2}\mu^2\omega_0^2\mathrm{Im}[G_\perp(\mathbf{r},\mathbf{r};\omega_0) - G_\parallel(\mathbf{r},\mathbf{r};\omega_0)] = \tfrac{1}{2}(\Gamma_\perp - \Gamma_\parallel). \tag{8}$$

Here $G_\perp(\mathbf{r},\mathbf{r};\omega_0) = G_{zz}(\mathbf{r},\mathbf{r};\omega_0)$, $G_\parallel(\mathbf{r},\mathbf{r};\omega_0) = G_{xx}(\mathbf{r},\mathbf{r};\omega_0)$ denote components of the EM Green's tensor where the symbol $\perp$ ($\parallel$) refers to a dipole-oriented normal (parallel) to the surface of the nanostructure. Finally, we define the

*vyannop@upatras.gr

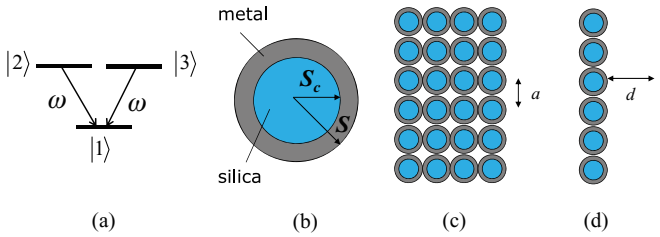

FIG. 1. (Color online) (a) A V-type, three-level system. (b) Metallic nanoshell made from a silica core of radius S_c and metal coating of thickness $S - S_c$. (c) Square lattice of metallic nanoshells (monolayer) with period a. (d) Side view of the monolayer, where d is the distance of the quantum emitter from the surface of a nanoshell.

spontaneous emission rates normal and parallel to the surface as $\Gamma_{\perp,\parallel} = \mu^2\omega_0^2 \mathrm{Im}[G_{\perp,\parallel}(\mathbf{r},\mathbf{r};\omega_0)]$. The degree of quantum interference is defined as $p = (\Gamma_\perp - \Gamma_\parallel)/(\Gamma_\perp + \Gamma_\parallel)$. For $p = 1$ we have maximum quantum interference. This can be achieved by placing the emitter close to a structure that completely quenches $\Gamma_\parallel$. We stress that when the emitter is placed in vacuum, $\Gamma_\perp = \Gamma_\parallel$ and $\kappa = 0$ ($p = 0$), so no quantum interference occurs in the system.

The EM Green's tensor which provides the corresponding spontaneous emission rates $\Gamma_\perp$ and $\Gamma_\parallel$ is given by [16,17]

$$G_{ii'}^{EE}(\mathbf{r},\mathbf{r}';\omega) = g_{ii'}^{EE}(\mathbf{r},\mathbf{r}';\omega) - \frac{i}{8\pi^2}\int\int_{\mathrm{SBZ}} d^2\mathbf{k}_\parallel \sum_{\mathbf{g}} \frac{1}{c^2 K_{\mathbf{g};z}^+} \times v_{\mathbf{g}\mathbf{k}_\parallel;i}(\mathbf{r}) \exp(-i\mathbf{K}_\mathbf{g}^+ \cdot \mathbf{r})\hat{\mathbf{e}}_{i'}(\mathbf{K}_\mathbf{g}^+), \quad (9)$$

with

$$v_{\mathbf{g}\mathbf{k}_\parallel;i}(\mathbf{r}) = \sum_{\mathbf{g}'} R_{\mathbf{g}';\mathbf{g}}(\omega,\mathbf{k}_\parallel) \exp(-i\mathbf{K}_{\mathbf{g}'}^- \cdot \mathbf{r})\hat{\mathbf{e}}_i(\mathbf{K}_{\mathbf{g}'}^-) \quad (10)$$

and

$$\mathbf{K}_\mathbf{g}^\pm = (\mathbf{k}_\parallel + \mathbf{g}, \ \pm[q^2 - (\mathbf{k}_\parallel + \mathbf{g})^2]^{1/2}). \quad (11)$$

The vectors $\mathbf{g}$ denote the reciprocal-lattice vectors corresponding to the two-dimensional periodic lattice of the plane of scatterers and $\mathbf{k}_\parallel$ is the reduced wave vector which lies within the surface Brillouin zone (SBZ) associated with the reciprocal lattice [18]. When $q^2 = \omega^2/c^2 < (\mathbf{k}_\parallel + \mathbf{g})^2$, $\mathbf{K}_\mathbf{g}^\pm$ defines an evanescent wave. The term $g_{ii'}^{EE}(\mathbf{r},\mathbf{r}';\omega)$ of Eq. (9) is the free-space Green's tensor and $\hat{\mathbf{e}}_i(\mathbf{K}_\mathbf{g}^\pm)$ the polar unit vector normal to $\mathbf{K}_\mathbf{g}^\pm$. $R_{\mathbf{g}';\mathbf{g}}(\omega,\mathbf{k}_\parallel)$ is the reflection matrix which provides the sum (over $\mathbf{g}$'s) of reflected beams generated by the incidence of plane wave from the left of the plane of scatterers [18]. Also, in Eq. (9) the terms corresponding to s-polarized waves (those containing components with the azimuthal unit vector $\hat{\mathbf{e}}_i(\mathbf{K}_\mathbf{g}^\pm)$ normal to $\mathbf{K}_\mathbf{g}^\pm$) have small contribution to the decay rates and therefore have been neglected.

The plasmonic nanostructure considered in this study is a two-dimensional array of touching metal-coated spherical dielectric (silica) nanoparticles and is shown in Figs. 1(b)–1(d). The dielectric function of the shell, $\epsilon_m(\omega)$, is provided by a Drude-type electric permittivity given by

$$\epsilon_m(\omega) = 1 - \frac{\omega_p^2}{\omega(\omega + i/\tau)}, \quad (12)$$

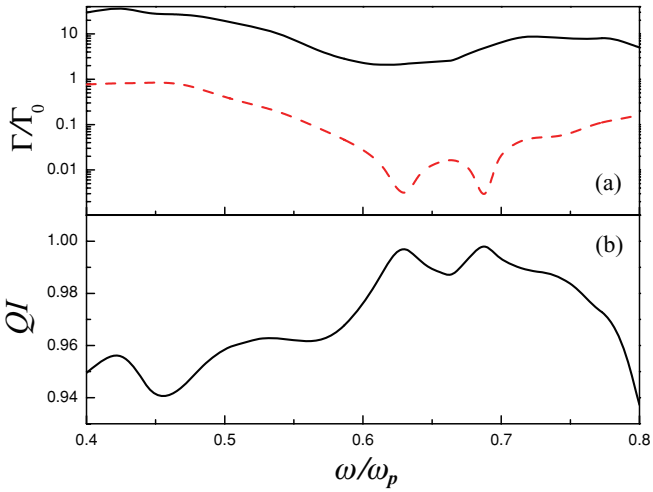

FIG. 2. (Color online) (a) The spontaneous decay rate as a function of the transition frequency close to a monolayer of plasmonic nanoshells with $(\omega_p\tau)^{-1} = 0.05$ for a dipole which is normally ($\Gamma_\perp$ – solid curve) and tangentially ($\Gamma_\parallel$ – dashed curve) oriented with respect to a plane of spheres. The quantum emitter is placed at a distance $d = 0.5c/\omega_p$ from the surface of a sphere of the plane. (b) The corresponding quantum interference factor p. Γ_0 is the decay rate in the vacuum.

where ω_p is the bulk plasma frequency and τ the relaxation time of the conduction-band electrons of the metal. The lattice constant of the square lattice is $a = 2c/\omega_p$ and the sphere radius $S = c/\omega_p$ with core radius $S_c = 0.7c/\omega_p$.

Figure 2 shows the spontaneous decay rates near the plasmonic nanostructure described above. This is calculated with the method analyzed in Refs. [16–19]. It is evident that $\Gamma_\parallel$ is suppressed relative to vacuum and exhibits significant suppression in the frequency region from $0.6\omega/\omega_p$ to $0.7\omega/\omega_p$, with the actual value becoming significantly smaller that the free space decay rate. In the same frequency region $\Gamma_\perp$ is also suppressed but it remains larger than the free space decay rate. In fact, for the the whole spectral range of Fig. 2, $\Gamma_\perp$ is much larger than $\Gamma_\parallel$ and the corresponding quantum interference factor p is above 0.935.

Initially, we study the case where only one of the upper states is initially excited, for example, $\rho_{22}(0) = 1$, $\rho_{33}(0) = 0$, $\rho_{23}(0) = 0$. The analytical formulas for the populations from Eqs. (1)–(3) are given by

$$\rho_{22}(t) = \tfrac{1}{4}(e^{-\Gamma_\parallel t} + e^{-\Gamma_\perp t})^2 \quad (13)$$

$$\rho_{33}(t) = \tfrac{1}{4}(e^{-\Gamma_\parallel t} - e^{-\Gamma_\perp t})^2. \quad (14)$$

An example of population dynamics for this case is shown in Fig. 3(a). As the population evolves in time population transfer to the initially unexcited is found. The population to each excited state becomes approximately 1/4 and it is followed by a very slow decay of the population. This is in contrast to the case that the quantum interference is zero, i.e., $\kappa = 0$, where the spontaneous decay rates are influenced, but the population of the initially excited state evolves exponentially with $\rho_{22}(t) = e^{-(\Gamma_\parallel + \Gamma_\perp)t}$, and the other state is not involved in the dynamics, $\rho_{33}(t) = 0$.

Then we consider the case where the upper states have initially equal population, i.e., $\rho_{22}(0) = \rho_{33}(0) = 1/2$ and

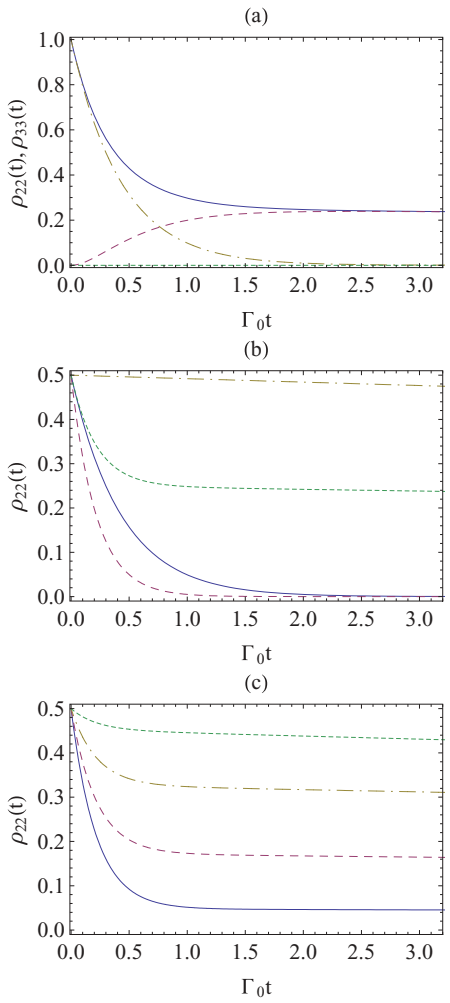

FIG. 3. (Color online) (a) Population dynamics of states $|2\rangle$ (solid curve with quantum interference and dot-dashed curve without quantum interference) and $|3\rangle$ (dashed curve with quantum interference and dotted curve without quantum interference), when the emitter is initially in state $|2\rangle$. (b) Population dynamics of state $|2\rangle$ without quantum interference (solid curve) and with quantum interference: symmetric superposition (dashed curve), antisymmetric superposition (dot-dashed curve), and complete incoherent mixture (dotted curve). (c) Population dynamics of state $|2\rangle$ for $C = e^{i\phi}$, and $\phi = \pi/5$ (solid curve), $\phi = 2\pi/5$ (dashed curve), $\phi = 3\pi/5$ (dot-dashed curve), $\phi = 4\pi/5$ (dotted curve). Here, $d = 0.5c/\omega_p$ and $\omega_0 = 0.64\omega_p$.

$\rho_{23}(0) = C/2$, where $0 \leqslant |C| \leqslant 1$ determines the initial quantum (atomic) coherence in the system. For $|C| = 1$ we have maximum quantum coherence, and $C = 1$ ($C = -1$) represents a symmetric (antisymmetric) superposition of the two excited states. For $C = 0$ we have a complete (uniform) incoherent mixture of the upper states. The analytical formulas for the populations from Eqs. (1)–(3) for this case are given by

$$\rho_{22}(t) = \rho_{33}(t) = \tfrac{1}{4}\{e^{-2\Gamma_\parallel t}[1 - \mathrm{Re}(C)] + e^{-2\Gamma_\perp t}[1 + \mathrm{Re}(C)]\}. \tag{15}$$

We note that the dynamics of the system is determined only by the real part of C. Therefore, a partially coherent initial state with C real will give the same population dynamics as a maximum coherent initial superposition with $\rho_{23}(0) = e^{i\phi}/2$, as long as $\cos\phi = C$.

For the case of the symmetric superposition

$$\rho_{22}(t) = \rho_{33}(t) = \tfrac{1}{2}e^{-2\Gamma_\perp t}, \tag{16}$$

for antisymmetric superposition

$$\rho_{22}(t) = \rho_{33}(t) = \tfrac{1}{2}e^{-2\Gamma_\parallel t}, \tag{17}$$

and for the complete incoherent mixture

$$\rho_{22}(t) = \rho_{33}(t) = \tfrac{1}{4}(e^{-2\Gamma_\parallel t} + e^{-2\Gamma_\perp t}). \tag{18}$$

An example of population dynamics for this case is shown in Fig. 3(b). For the case of the symmetric superposition, the population decays faster than for the absence of quantum interference, where $\rho_{22}(t) = \rho_{33}(t) = \frac{1}{2}e^{-(\Gamma_\parallel + \Gamma_\perp)t}$, as the population dynamics is determined solely by $\Gamma_\perp$ that is enhanced. In contrast, for the case of the antisymmetric superposition a very slow population decay is found as the decay is determined solely by $\Gamma_\parallel$ that is significantly suppressed. For the case of the incoherent mixture, two different decay evolutions are found, an initial fast response determined by $\Gamma_\perp$ and a forthcoming very slow response determined by $\Gamma_\parallel$. This population response also occurs for different values of C as well, as can be seen from Eq. (15) and Fig. 3(c). It is clear that the actual population dynamics depends strongly on C.

In summary, we have studied the effects of the presence of a two-dimensional array of metal-coated dielectric nanospheres on the decay rates and the population dynamics of a V-type quantum emitter placed near the plasmonic nanostructure. We show that the decay rate of a perpendicular oriented dipole, relative to the surface of the nanostructure, is enhanced while the decay rate of a parallel-oriented dipole is significantly suppressed. We then analyze the population dynamics of the system for different initial conditions. We show that when only a single upper state is initially excited then via quantum interference the other excited state is also populated, and both states obtain the same population as time evolves. This population is slowly decaying for the case that the transition frequency of the quantum emitter is in the frequency region where the decay rate of the parallel oriented dipole is significantly suppressed. For the same frequency region, both excited states having initially the same population leads to a quite different response, depending on the initial quantum coherence. For the case of an initial symmetric superposition fast population decay is found, while for the case of an initial antisymmetric superposition a significantly slow population decay is predicted. Finally, for the case of an initial incoherent mixture it is found that an initial fast population decay is followed by a very slow population decay.

This research has been co-financed by the European Union (European Social Fund - ESF) and Greek national funds through the Operational Program "Education and Lifelong Learning" of the National Strategic Reference Framework (NSRF) - Research Funding Program: Heracleitus II. Investing in knowledge society through the European Social Fund.

[1] V. V. Klimov, M. Ducloy, and V. S. Letokhov, Quantum Electron. **31**, 569 (2001).
[2] S. Kühn, G. Mori, M. Agio, and V. Sandoghdar, Mol. Phys. **106**, 893 (2008).
[3] G. S. Agarwal, Phys. Rev. Lett. **84**, 5500 (2000).
[4] S.-Y. Zhu, R. C. F. Chan, and C. P. Lee, Phys. Rev. A **52**, 710 (1995).
[5] S.-Y. Zhu and M. O. Scully, Phys. Rev. Lett. **76**, 388 (1996).
[6] P. Zhou and S. Swain, Phys. Rev. Lett. **77**, 3995 (1996).
[7] E. Paspalakis and P. L. Knight, Phys. Rev. Lett. **81**, 293 (1998).
[8] E. Paspalakis, C. H. Keitel, and P. L. Knight, Phys. Rev. A **58**, 4868 (1998).
[9] P. R. Berman, Phys. Rev. A **58**, 4886 (1998).
[10] C. H. Keitel, Phys. Rev. Lett. **83**, 1307 (1999).
[11] M. Macovei and C. H. Keitel, Phys. Rev. Lett. **91**, 123601 (2003).
[12] S. E. Economou, R. B. Liu, L. J. Sham, and D. G. Steel, Phys. Rev. B **71**, 195327 (2005).
[13] M. A. Antón, O. G. Calderón, and F. Carreño, Phys. Rev. A **72**, 023809 (2005).
[14] C.-L. Wang, Z.-H. Kang, S.-C. Tian, Y. Jiang, and J.-Y. Gao, Phys. Rev. A **79**, 043810 (2009).
[15] For a recent review see M. Kiffner, M. Macovei, J. Evers, and C. H. Keitel, in *Progress in Optics*, edited by E. Wolf, Vol. 55 (Elsevier, Amsterdam, 2010), p. 85.
[16] V. Yannopapas, E. Paspalakis, and N. V. Vitanov, Phys. Rev. Lett. **103**, 063602 (2009).
[17] R. Sainidou, N. Stefanou, and A. Modinos, Phys. Rev. B **69**, 064301 (2004).
[18] N. Stefanou, V. Yannopapas, and A. Modinos, Comput. Phys. Commun. **113**, 49 (1998); **132**, 189 (2000).
[19] V. Yannopapas and N. V. Vitanov, Phys. Rev. B **75**, 115124 (2007).
[20] A. Hatef and M. R. Singh, Phys. Rev. A **81**, 063816 (2010).
[21] D. E. Chang, A. S. Sorensen, P. R. Hemmer, and M. D. Lukin, Phys. Rev. Lett. **97**, 053002 (2006); D. E. Chang *et al.*, Nat. Phys. **3**, 807 (2007).
[22] V. Yannopapas and N. V. Vitanov, J. Phys. Condens. Matter **19**, 096210 (2007).
[23] Y.-N. Chen, G.-Y. Chen, D.-S. Chuu, and T. Brandes, Phys. Rev. A **79**, 033815 (2009).
[24] A. Trügler and U. Hohenester, Phys. Rev. B **77**, 115403 (2008).
[25] Y. Gu, L. Huang, O. J. F. Martin, and Q. Gong, Phys. Rev. B **81**, 193103 (2010).
[26] R. Marty, A. Arbouet, V. Paillard, C. Girard, and G. Colas des Francs, Phys. Rev. B **82**, 081403(R) (2010).
[27] A. Gonzalez-Tudela, F. J. Rodriguez, L. Quiroga, and C. Tejedor, Phys. Rev. B **82**, 115334 (2010).
[28] D. Dzsotjan, A. S. Sorensen, and M. Fleischhauer, Phys. Rev. B **82**, 075427 (2010).
[29] G. X. Li, F.-L. Li, and S.-Y. Zhu, Phys. Rev. A **64**, 013819 (2001).
[30] Y.-P. Yang, J.-P. Xu, H. Chen, and S.-Y. Zhu, Phys. Rev. Lett. **100**, 043601 (2008).
[31] G.-X. Li, J. Evers, and C. H. Keitel, Phys. Rev. B **80**, 045102 (2009).
[32] J.-P. Xu and Y.-P. Yang, Phys. Rev. A **81**, 013816 (2010).
[33] J.-P. Xu, L.-G. Wang, Y.-P. Yang, Q. Lin, and S.-Y. Zhu, Opt. Lett. **33**, 2005 (2008).